

# Properties of the metallic phase of zinc-doped platinum catalysts for propane dehydrogenation

Changlin Yu, Hengyong Xu<sup>\*</sup>, Qingjie Ge, Wenzhao Li

*Applied Catalysis Laboratory, Dalian Institute of Chemical Physics, Graduate School of the Chinese Academy of Sciences, 457 Zhongshan Road, Dalian 116023, China*

Received 13 May 2006; received in revised form 11 October 2006; accepted 15 October 2006  
Available online 20 October 2006

## Abstract

The influence of the zinc addition to alumina supported Pt and PtSn catalysts is analyzed in this paper, not only on the activity, selectivity and deactivation in the propane dehydrogenation reaction, but also on the characteristics of platinum metal phase. Zinc can give a remarkable improvement in dehydrogenation performance of catalysts. High propylene selectivity ( $\geq 97\%$ ) can be obtained over zinc-doped catalysts. Physicochemical technologies like BET,  $\text{NH}_3$ -TPD,  $\text{H}_2$ -TPR,  $\text{H}_2$ -chemisorption,  $\text{C}_3\text{H}_6$ -TPD, CO-FTIR and TPO were used to characterize the metal phase of catalysts. The presence of zinc modifies the metallic phase, mainly by geometric and electronic modifications of the metallic phase. These modifications could be responsible for the improvement of catalytic performance.

© 2006 Elsevier B.V. All rights reserved.

**Keywords:** Platinum catalyst; Zinc effect; Propane dehydrogenation to propylene

## 1. Introduction

Catalytic dehydrogenation processes are of increasing importance because of growing demand for light olefins such as propylene and isobutene. Supported platinum is a good catalyst for reforming and dehydrogenation reactions. Addition of Sn to Pt/ $\text{Al}_2\text{O}_3$  naphtha-reforming catalysts is well known to promote desired dehydrogenation reactions and inhibit coking reactions [1–3].

The role of Sn in PtSn catalysts has been extensively investigated in many studies [4–11]. The effect of tin has been explained in terms of geometric effect and/or electronic effect [12]. *Geometric effect:* tin decreases the size of platinum ensembles, reducing hydrogenolysis and coking reactions that require large platinum ensembles. *Electronic effect:* tin modifies the electronic density of Pt, either due to a positive charge transfer from  $\text{Sn}^{n+}$  species or to the different electronic structures in PtSn alloys [13]. The dehydrogenation performance of PtSn catalysts depends on the Sn/Pt atomic ratio, the preparation method and, especially, the interactions between platinum and tin species.

Since the dehydrogenation of propane to propylene is an endothermic reaction, temperatures in excess of  $550^\circ\text{C}$  are needed to obtain high conversions. However, the rate of hydrogenolysis and coking reactions becomes significant at these high temperatures. Accordingly, the selectivity toward dehydrogenation becomes low at high temperatures required for favorable dehydrogenation thermodynamics. Although great efforts have been made to improve the stability, selectivity and activity of PtSn catalysts by the addition of some alkali metals such as Li, Ba, K, Ca and others, or by the utilization of non-acidic and thermal stable supports such as  $\text{MgAl}_2\text{O}_4$  and  $\text{ZnAl}_2\text{O}_4$  [14,15], the dehydrogenation performance of PtSn catalysts is still not satisfactory, especially regarding the stability and selectivity of the catalysts. Therefore, it is necessary to further improve the catalytic performance of PtSn catalysts during light paraffin conversion.

Addition of Zn to Pt-based catalysts can lead to an obvious change of catalytic performance. For example, the addition of Zn to Pt/ $\text{Al}_2\text{O}_3$  catalysts can promote the selective reduction of NO [16] and improve the resistance of these systems in waste gas treatment processes [17]. It has been reported that over Pt/ZnO catalysts high hydrogenation and dehydrogenation selectivity could be obtained [18,19]. These

<sup>\*</sup> Corresponding author. Tel.: +86 411 84581234; fax: +86 411 84581234.  
E-mail address: [xuhy@dicp.ac.cn](mailto:xuhy@dicp.ac.cn) (H. Xu).

performance changes are mainly attributed to the strong interactions between Zn and Pt which result in the formation of PtZn alloy and the change in electronic property of Pt atom (e.g., the formation of  $\text{Pt}^{\delta-}-\text{Zn}^{\delta+}$  entities). It appears that Zn causes similar effects to Sn for the modification of Pt catalysts in dehydrogenation processes. However, comparatively few studies about the effects of zinc on alumina supported platinum catalysts in propane dehydrogenation were reported.

In this paper, the influence of the Zn addition to alumina supported Pt and PtSn catalysts on the activity, selectivity and deactivation in the propane dehydrogenation reaction is analyzed. Besides, a more detailed study of the effect of the Zn addition to alumina supported Pt and PtSn catalysts on the characteristics and properties of metallic phase is reported.

## 2. Experimental

### 2.1. Catalyst preparation

A commercial  $\gamma\text{-Al}_2\text{O}_3$  ( $S_{\text{BET}}: \geq 250 \text{ m}^2 \text{ g}^{-1}$ ), previously calcined in air at  $550^\circ\text{C}$  for 4 h and 40–60 mesh sieved, was used as support. Pt/ $\gamma\text{-Al}_2\text{O}_3$  catalyst was prepared by impregnating with excess aqueous solution of the Pt precursor ( $\text{H}_2\text{PtCl}_6$ ). After the impregnation, the catalyst was dried at  $110^\circ\text{C}$  overnight and then calcined at  $500^\circ\text{C}$  in air for 4 h. For Sn–Pt/ $\gamma\text{-Al}_2\text{O}_3$  and Zn–Pt/ $\gamma\text{-Al}_2\text{O}_3$  catalysts, Sn or Zn was first deposited by impregnating with  $\text{SnCl}_2$  ethanol solution or  $\text{Zn}(\text{NO}_3)_2$  aqueous solution, followed by drying and calcination, and finally the Pt component was added from aqueous Pt solution in a similar way. In the case of trimetallic catalysts, different impregnation orders were used. The trimetallic catalysts were designated by the names of the metal elements (Zn, Sn and Pt) separated by hyphens (-) and arranged in the order in which they were impregnated, dried and calcined. For example, Zn–Sn–Pt/ $\gamma\text{-Al}_2\text{O}_3$  is a trimetallic catalyst prepared by successive steps of: (i) impregnation of  $\gamma\text{-Al}_2\text{O}_3$  with an aqueous solution of the Zn precursor; (ii) drying and calcination; (iii) impregnation with an ethanol solution of the Sn precursor; (iv) drying and calcination; (v) impregnation with an aqueous solution of the Pt precursor; (vi) drying and calcination. Normally, the loadings of Pt, Sn and Zn were 0.3, 0.9 and 0.5 wt.%, respectively.

### 2.2. Activity test

Catalysts were tested in the propane dehydrogenation reaction in a flow reactor at atmospheric pressure. A sample (0.3 g), placed in a quartz fixed-bed reactor, was previously reduced under flowing pure  $\text{H}_2$  (12.6 ml/min) at  $576^\circ\text{C}$  for 2.5 h. Then the reaction mixture composed of  $\text{H}_2$ ,  $\text{C}_3\text{H}_8$  and Ar ( $\text{H}_2/\text{C}_3\text{H}_8/\text{Ar}$  molar ratio = 1:1:5) was fed to the reactor. The total GHSV was  $3800 \text{ h}^{-1}$ . Five minutes after beginning of the reaction, the gas compositions of reactant and products were analyzed by an FID gas chromatographic system (Shimadzu GC14-C) with a Porapak-Q packed column.

### 2.3. Catalyst characterizations

#### 2.3.1. Surface area measurements

The surface area of catalysts was measured on an automatic analyzer (NOVA 4000, Quantachrome, USA). The samples were outgassed for 1 h under vacuum at  $300^\circ\text{C}$ , prior to adsorption.

#### 2.3.2. Temperature-programmed desorption of ammonia

The acid properties of zinc-doped Pt and PtSn catalysts were determined by  $\text{NH}_3$ -TPD on an ASAP 2010C chemisorption analyzer. Samples (0.2 g) were placed into a quartz U-type reactor between two quartz wool plugs. The samples were treated by flowing dry argon (99.99%) at  $500^\circ\text{C}$  for 1 h prior to adsorption of ammonia. Then, samples were saturated by an ammonia pulse at room temperature. Before the run, the baseline was stabilized in dry argon (30 ml/min) at the same temperature for 2 h. Subsequently, the temperature was raised up to  $600^\circ\text{C}$  with a heating rate of  $10^\circ\text{C}/\text{min}$ . The  $\text{NH}_3$  desorption profile was observed with a thermal conductivity detector.

#### 2.3.3. Temperature-programmed reduction of hydrogen

All catalysts were characterized by temperature programmed reduction (TPR) on a conventional setup, consisting of a programmable temperature furnace and a chromatographic system (Shimadzu GC-8A). Before TPR experiment, the catalysts (0.08 g) were treated in situ by flowing dry Ar at  $500^\circ\text{C}$  for 1 h, and after cooled down to room temperature, the furnace was heated to  $800^\circ\text{C}$  at a rate of  $10^\circ\text{C}/\text{min}$  in 5%  $\text{H}_2/\text{Ar}$  stream (30 ml/min). The apparatus was calibrated by the reduction of CuO.

#### 2.3.4. Pulse chemisorption of hydrogen

Platinum dispersions were determined by pulse  $\text{H}_2$ -chemisorption. Pulse chemisorption of hydrogen experiments were carried out in the same setup as  $\text{H}_2$ -TPR. Samples (0.2 g) were previously reduced under flowing pure  $\text{H}_2$  (12.6 ml/min) at  $576^\circ\text{C}$  for 2.5 h, and then purged in Ar at  $550^\circ\text{C}$  for 2 h and cooled to  $25^\circ\text{C}$ . The pulse size was 0.32 ml 5% (v/v)  $\text{H}_2$  in Ar mixture and the time between pulses was 3 min.

#### 2.3.5. Fourier transform infrared spectroscopy of CO adsorption

The electronic property of the metallic phase was measured by CO adsorption on an FTIR spectrometer (EQUINOX55) with a Pyrex glass IR cell equipped with  $\text{CaF}_2$  windows, using 64 scans for each spectrum. Catalysts were compressed to disks ( $\varnothing$  1 cm, about 15 mg) which were placed in the sample holder of the IR cell. This IR cell enabled in situ treatments ( $0\text{--}500^\circ\text{C}$ ) of the solid with a gas flow at atmospheric pressure. Prior to CO adsorption, the samples were reduced under a flow of  $\text{H}_2$  (50 ml/min) for 90 min at  $400^\circ\text{C}$ . After the sample was cooled to room temperature in the flow of  $\text{H}_2$ , the IR cell was evacuated to  $2 \times 10^{-2} \text{ Pa}$  for 6 h. Then CO was introduced into the cell (CO pressure:  $2.7 \times 10^3 \text{ Pa}$ ) and the CO pressure was maintained for 1 h at  $25^\circ\text{C}$ . The excess of CO was evacuated and the CO adsorption spectra were recorded. The adsorptions by the

windows and by the blank powdered sample were subtracted from all the spectra.

### 2.3.6. $C_3H_6$ -TPD measurements

The property of metallic phase to adsorb propylene was measured by  $C_3H_6$ -TPD on an ASAP 2010C chemisorption analyzer. Samples (0.35 g) were reduced under flowing pure  $H_2$  at  $576^\circ C$  for 2.5 h, then purged in flowing dry Ar at  $580^\circ C$  for 2 h and cooled to  $20^\circ C$ . The catalysts were kept in the pure propylene gas flow for 30 min at  $20^\circ C$ , and then the catalysts were washed with flowing dry Ar for 1 h. The temperature was ramped up at  $6^\circ C/min$  while the generated products were monitored by an on-line mass spectrometer (Omnisorp. Corp.)

### 2.3.7. Coke analysis

Coke was analyzed by TPO and  $O_2$ -pulse experiments.  $O_2$ -pulse experiment is a special technology used for quantitative coke analysis. In TPO experiments, the used samples (0.2 g) were purged in a He flow (40 ml/min) at  $500^\circ C$  for 30 min and then the temperature lowered to  $25^\circ C$  prior to the TPO in a 2 vol.% oxygen/98 vol.% helium mixture flow of 40 ml/min. The temperature was ramped up at  $10^\circ C/min$  while the  $CO_2$  generated was monitored by an on-line mass spectrometer (Omnisorp. Corp.). The pulse experiments were carried out at  $800^\circ C$  by injecting pulses of pure  $O_2$  (99.99%) to the coke deposited catalysts (0.03 g), which was maintained under flowing pure Ar between two successive pulses. The  $CO_2$  generated was continuously monitored with a TCD cell and recorded. Pulses of pure  $O_2$  stopped until deposited carbon entirely converted to  $CO_2$ . Then the amount of generated  $CO_2$  was converted to the amount of deposited coke on catalyst.

## 3. Results and discussion

### 3.1. Activity test in propane dehydrogenation

#### 3.1.1. Effect of zinc addition to Pt and PtSn catalysts

Table 1 shows the effect of zinc addition to Pt and PtSn catalysts on the catalytic performance in the propane dehydrogenation reaction at  $576^\circ C$ . A deactivation parameter  $D$  (defined as  $D = [X_0 - X_f] \times 100\% / X_0$ , where  $X_0$  is the initial propane conversion and  $X_f$  is the final propane conversion) is used to characterize the activity maintenance.  $S_0$  and  $S_f$  are the initial and final selectivities to propylene, respectively. It can be seen that all catalysts show activity decay with respect to time-on-stream. The initial conversions of propane catalyzed by

Table 1  
Values of initial conversion obtained at 5 min of reaction ( $X_0$ ), deactivation parameter defined as  $[(X_0 - X_f)/X_0 \times 100]$ ;  $X_f$  is the final conversion, initial selectivity ( $S_0$ ) and final selectivity ( $S_f$ ) to propylene

Catalyst	$X_0$ (%)	$X_f$ (%)	$(X_0 - X_f)/X_0$ (%)	$S_0$ (%)	$S_f$ (%)
Pt/Al	34.1	18.6	45	79.2	90.1
Sn–Pt/Al	42.3	32.5	23	88.1	95.8
Zn–Pt/Al	37.3	24.2	35	97.2	98.9
Zn–Sn–Pt/Al	42.5	40.3	5	98.0	99.0

Reaction temperature:  $576^\circ C$ .

Table 2

Effect of metal deposition sequence on the activity, selectivity and deactivation of dehydrogenation

Catalyst	$X_0$ (%)	$X_f$ (%)	$(X_0 - X_f)/X_0$ (%)	$S_0$ (%)	$S_f$ (%)
ZnSn–Pt/Al	44.7	40.5	9	86.9	95.0
Pt–ZnSn/Al	40.2	37.2	7	98.5	99.2
Sn–Zn–Pt/Al	41.4	39.0	6	97.2	98.8
Sn–Pt–Zn/Al	38.3	30.4	21	97.7	98.8

Reaction temperature:  $576^\circ C$ .

Pt/Al, Sn–Pt/Al, Zn–Pt/Al, and Zn–Sn–Pt/Al catalysts are 34.1, 42.3, 37.3, and 42.5%, respectively. The values of  $D$  for Pt/Al, Sn–Pt/Al, Zn–Pt/Al, and Zn–Sn–Pt/Al catalysts are 45, 23, 35, and 5%, respectively. Although addition of Zn to Pt/Al results in only a small increase in conversion of propane, Zn gives a rapid increase in selectivity towards propylene. Over the zinc-doped PtSn catalyst an overall improvement in catalytic performance is obtained. The Zn–Sn–Pt/Al catalyst exhibits the lowest deactivation value (5%) and the highest initial propylene selectivity (98.8%). The value of  $D$  over the Zn–Sn–Pt/Al catalyst is lower than 80% of the value over the Sn–Pt/Al catalyst. The initial and final yields of propylene can reach as high as 41.7 and 39.9%, respectively.

#### 3.1.2. Effect of zinc deposition sequence

The effect of zinc deposition sequence on the dehydrogenation performance was investigated and the results are shown in Table 2. Clearly, the sequence of zinc deposition can strongly influence the catalytic performance. The highest initial conversion of propane (44.7%) is obtained over the SnZn–Pt/Al catalyst, while its selectivity to propylene is the lowest (initial: 86.9%; final: 95.0%). The highest selectivity towards propylene is observed over Pt–SnZn/Al (initial: 98.5%; final: 99.2%), which means the cracking reactions hardly take place on the Pt–SnZn/Al catalyst. The Sn–Pt–Zn/Al catalyst exhibits the highest deactivation value (20%). Over the Zn–Sn–Pt/Al and Sn–Zn–Pt/Al catalysts, the deactivation values are almost the same (5 and 6%, respectively), but the conversion of propane over the Zn–Sn–Pt/Al catalyst (initial: 42.5%; final 40.3%) is slightly higher than that over the Sn–Zn–Pt/Al catalyst (initial: 41.4%; final 39.0%).

#### 3.1.3. Effect of zinc content

Zinc content influence on the catalytic performance of Zn–Sn–Pt/Al was measured and the results are shown in Fig. 1. The zinc content greatly influences not only the stability of catalyst but also the dehydrogenation activity. With the increase in the zinc content, a gradual increase in selectivity towards propylene appears. But, when zinc loading increases to 1.0 wt.%, the catalyst suffers severe activity loss. The deactivation value increases to as high as 28%. The optimal zinc loading is about 0.5%.

### 3.2. Characterization of the metallic phase

#### 3.2.1. Surface area and Pt dispersion

Table 3 shows the specific surface area and platinum dispersion of catalysts. Platinum dispersion was calculated from

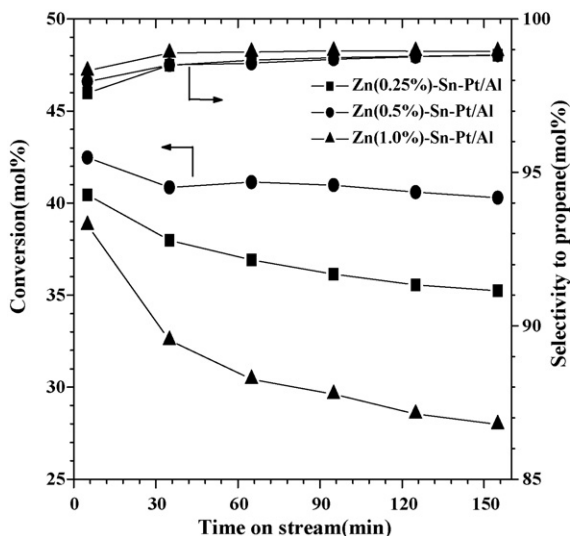


Fig. 1. Effect of zinc content on catalytic dehydrogenation performance of Zn-Sn-Pt/Al catalyst at 576 °C.

hydrogen pulse chemisorption at 25 °C using the assumption H:Pt=1 [20,21]. The specific surface area of the Zn-Pt/Al catalyst is smaller than that of the Pt/Al catalyst. The presence of Zn must plug some of the pores of the Al<sub>2</sub>O<sub>3</sub> support and thereby causes a slight decrease in pore volume with a concomitant loss of surface area. Regarding zinc-doped PtSn catalysts, although the specific surface area of the Zn-Sn-Pt/Al and Sn-Zn-Pt/Al catalysts is slightly higher than that of the Sn-Pt/Al catalyst, the existence of zinc dose not result in practical change in surface area. In the case of platinum dispersion, an obvious increase in platinum dispersion is observed over both Zn doped Pt/Al and Zn doped PtSn catalysts. Over Zn doped PtSn catalysts, platinum dispersion is also influenced by the zinc deposition order. Low platinum dispersion appears over the Sn-Zn-Pt/Al and Pt-SnZn/Al catalysts. Considering the surface area of the Sn-Pt catalyst is almost the same as that of the zinc-doped PtSn catalysts, the reasons for the increase in platinum dispersion in trimetallic catalysts would likely be that interactions between Pt, Sn and Zn three components affect either the degree of Pt sintering during calcination or the properties of the surface of platinum metal. Different zinc deposition order may result in the appearance of different interactions. Looking at the activity test, the existence of zinc in Pt and PtSn catalysts can notably promotes the sta-

bility and selectivity of dehydrogenation, which can be partly attributed to the increase in platinum dispersion. Previous studies have shown that the active site for propane dehydrogenation to propylene is the single platinum atom, while hydrogenolysis and coke reactions need the large platinum particles [22]. Furthermore, zinc can act as spacer to reduce the size of the platinum particles as the role of tin in PtSn catalyst [7,23] and suppress the undesired reactions which need large platinum ensembles.

### 3.2.2. The acidity of catalysts

The acidity of catalysts strongly affects their performance of dehydrogenation. The effects of zinc on the acidity of the Pt/Al and PtSn/Al catalysts were determined by NH<sub>3</sub>-TPD. From Fig. 2, it can be seen that over all samples a broad desorption peak with a maximum at 172–182 °C and a shoulder at higher temperatures (260–290 °C) can be visible. The low temperatures peak can be ascribed to weak and medium strength acid sites, whereas peak above 260 °C is typical of strong acid sites. Over the Zn-Pt/Al catalyst, although the total amount of acidity (calculate from the total desorption peak area) is higher than that over Pt/Al, the strong acid sites of the alumina are poisoned by zinc. For the zinc-doped PtSn catalysts, there are no obvious changes in acidity due to the presence of zinc. In dehydrogenation reaction, side reactions (cracking, isomerization and polymerization) are mainly catalyzed by strong acid centers. Thereby, the destruction of strong acid centers by zinc will minimize the undesirable side reactions and promote the selectivity to propylene. However, it must be noticed that for the Zn-Sn-Pt/Al catalyst, the improvement in selectivity can not be totally attributed to the changes in acidity because its acidity is almost the same as that of the Sn-Pt/Al catalyst. Other important reasons for the improvement in catalytic performance should be made clear.

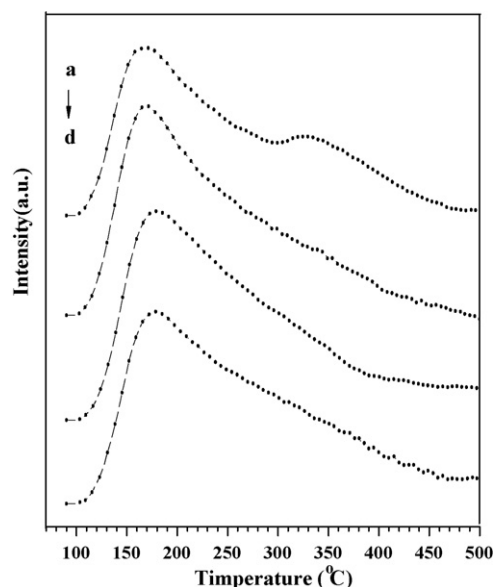


Fig. 2. NH<sub>3</sub>-TPD profiles of the catalysts. (a) Pt/Al; (b) Sn-Pt/Al; (c) Zn-Pt/Al; (d) Zn-Sn-Pt/Al.

Table 3  
Surface area and Pt dispersion of the catalysts

Catalyst	Specific area (m <sup>2</sup> /g)	Pt dispersion
Pt/Al	250	0.16
Sn-Pt/Al	213	0.41
Zn-Pt/Al	229	0.36
Zn-Sn-Pt/Al	224	0.68
Sn-Pt-Zn/Al	212	0.69
Sn-Zn-Pt/Al	228	0.59
Pt-SnZn/Al	212	0.40
SnZn-Pt/Al	210	0.65

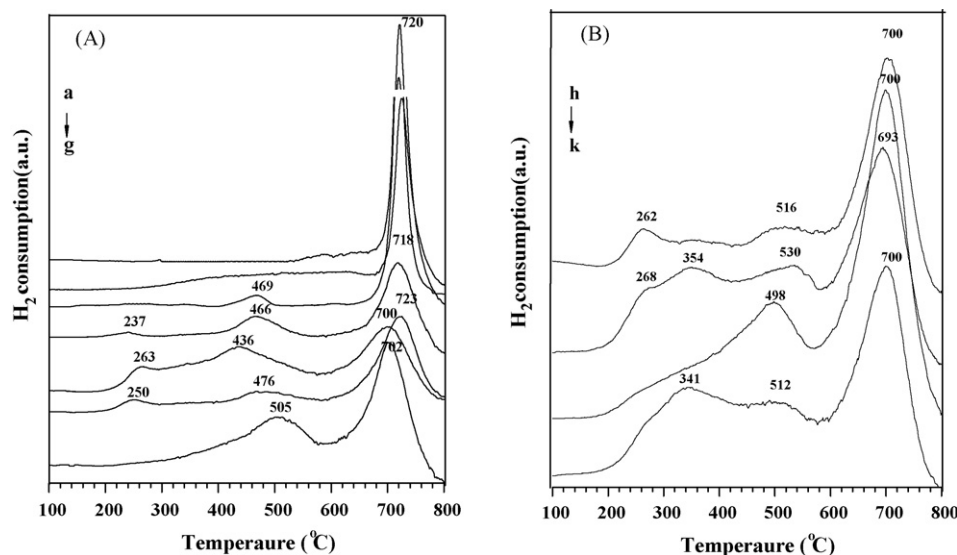


Fig. 3. H<sub>2</sub>-TPR profiles of the samples. (A) a: Al<sub>2</sub>O<sub>3</sub>; b: Sn/Al; c: Zn/Al; d: Pt/Al; e: Sn–Pt/Al; f: Zn–Pt/Al; g: Zn–Sn–Pt/Al. (B) h: Sn–Pt–Zn/Al; i: Sn–Zn–Pt; j: SnZn–Pt/Al; k: Pt–SnZn/Al.

### 3.2.3. TPR analysis

The influences of zinc on the reduction properties of the Pt/Al and PtSn/Al catalysts were measured by TPR. The TPR profiles of all samples are shown in Fig. 3. Table 4 shows the estimate of metal reduction extent in some samples, measured during H<sub>2</sub>-TPR experiments.  $\text{PtO}_2 + 2\text{H}_2 \rightarrow \text{Pt}^0 + 2\text{H}_2\text{O}$ ,  $\text{SnO}_2 + 2\text{H}_2 \rightarrow \text{Sn}^0 + 2\text{H}_2\text{O}$  and  $\text{ZnO} + \text{H}_2 \rightarrow \text{Zn}^0 + \text{H}_2\text{O}$  were the stoichiometry considered for Pt, Sn and Zn reduction, as described in literatures [24,25].

All samples show a sharp reduction peak at about 700 °C. The origin of the 700 °C peak is not clearly known, but it is speculated that it is linked with the reduction of OH groups or alumina ions in the surface of support. When Pt is present, this peak shifts to low temperatures and becomes broad. Over the Sn/Al sample, Sn shows low reducibility, as indicated by the small broad peaks from 250 to 640 °C. The average degree of Sn reduction is esti-

Table 4  
Degrees of reduction calculated from hydrogen consumption in the TPR experiment

Sample	Degree of reduction (%)		
	Pt <sup>a</sup>	Sn <sup>b</sup>	Zn <sup>c</sup>
Pt/Al	98	–	–
Sn/Al	–	15	–
Zn/Al	–	–	41
Sn–Pt/Al	100 <sup>d</sup>	48	–
Zn–Pt/Al	100 <sup>d</sup>	–	73

<sup>a</sup> Measured from the hydrogen consumption assuming the reaction  $\text{PtO}_2 + 2\text{H}_2 \rightarrow \text{Pt}^0 + 2\text{H}_2\text{O}$ , corrected for the consumption over the support alone.

<sup>b</sup> Measured from the hydrogen consumption assuming the reaction  $\text{SnO}_2 + 2\text{H}_2 \rightarrow \text{Sn}^0 + 2\text{H}_2\text{O}$ , corrected for the reduction of Pt and the support alone.

<sup>c</sup> Measured from the hydrogen consumption assuming the reaction  $\text{ZnO} + \text{H}_2 \rightarrow \text{Zn}^0 + \text{H}_2\text{O}$ , corrected for the reduction of Pt and the support alone.

<sup>d</sup> 100% reduction of Pt assumed when calculating the degree of Sn and Zn reduction.

ated at about 15% as shown in Table 4, which implies the strong interactions between tin oxides and support alumina. Over the Zn/Al sample, a reduction peak appears around 469 °C, which must be attributed to the reduction of zinc species dispersed over alumina as reported in literature [26]. Over the Pt/Al catalyst, two reduction peaks appear, one near 237 °C and another around 466 °C. Generally speaking, over Pt/Al<sub>2</sub>O<sub>3</sub> samples, two types of Pt oxides are considered in literatures [27–29], one in weak interaction with the support and the other in strong interaction. The former is reduced at low temperatures and the latter requires higher temperatures. Therefore, we can associate the hydrogen consumption peaks at 237 and 466 °C with the reduction of two kinds of platinum species. The average degree of Pt reduction is about 98% as shown in Table 2, which means that most of platinum species must be reduced to Pt<sup>0</sup> during the course of TPR experiment.

In the case of the Sn–Pt/Al catalyst, two low temperatures reduction peaks are present, one at 263 °C, and the other at 436 °C. These two reduction peaks must be related to the joint reduction of platinum and tin particles. The amounts of hydrogen consumption over the Sn–Pt/Al catalyst confirm that Pt assists the reduction of SnO<sub>2</sub>, as reported by others [4,6,30]. The average degree of Sn reduction is about 48%, which suggests that tin is to a large extent stabilized in the +2 state, as reported in literatures [25,31,32]. For the Zn–Pt/Al catalyst, the reduction peaks show similarities to those over Pt/Al. But, the amounts of hydrogen consumption show that the average reduction degree of Zn increases to 73% (Table 4), which is much higher than that over the Zn/Al catalyst (about 41%). This implies that there is a possibility of existence of PtZn alloy. Consonni [19] have reported that, over Pt/ZnO sample even at low reduction temperatures (200 °C), ZnO can be reduced to metallic Zn and lead to the formation of PtZn alloy. Addition of zinc to the PtSn catalyst, for Zn–Sn–Pt/Al catalyst, causes an obvious change in the TPR profile. Only one large reduction peak appears in the low temperatures region, and moves up to higher temperatures, around



505 °C. It is difficult to ascribe this peak correctly in this complicated trimetallic system. We cannot ascribe this major peak to the reduction of certain species. So, it must be reasonable to assign this peak to the conjunct reduction of platinum, tin and zinc species. Obviously, the reduction property of the PtSn catalyst is changed by the presence of zinc. The TPR profile of Zn–Sn–Pt/Al also indicates that strong interactions between zinc, tin and platinum three components may take place. It is very hard to calculate the average reduction degree of each metal over the complicated system using the former method.

The effect of zinc deposition on the reduction property of the PtSn catalyst is shown in Fig. 3(B). The TPR profile of the Sn–Pt–Zn/Al catalyst shows some similarities to that of the Zn–Pt/Al catalyst. Two major low temperatures reduction peaks appear, one near 262 °C and the other around 516 °C. When Sn is deposited firstly, Sn may firstly strongly interact with the support and has less chance to strongly interact with Pt. However, Zn must have more chance to interact with Pt. Therefore, the Sn–Pt–Zn/Al catalyst exhibits similar reduction properties to the Zn–Pt/Al catalyst. A decrease in the interactions between Pt and Sn may reduce the stability of catalyst, as indicated in propane dehydrogenation. Similarly, when metal is deposited in the order of Sn → Zn → Pt, Sn may firstly block the sites of the support, which results in fewer possibilities of Zn to affect the property of the support. But, its interaction with zinc must be weak and may be displaced by the noble platinum oxide. Thereby, over Sn–Zn–Pt/Al, the strong interactions between Pt and Sn may also emerge and it shows a reduction property similar to that of the Sn–Pt/Al catalyst. The profiles of the SnZn–Pt/Al and Zn–Sn–Pt/Al catalyst also show some similarities. For the Pt–SnZn/Al catalyst, when Pt precursor is added firstly, and Zn and Sn precursors added lastly, Pt may strongly interact with the support and lead to a decrease in interactions between Pt and promoters. The profiles of TPR imply that the zinc deposition order mainly influence the surface interactions between active sites, promoters, and support, which result in the difference in catalytic performance.

The above discussion indicates that the zinc influence on the catalysts reduction property is obvious. Over the Zn–Pt/Al catalyst, part of Zn species must be reduced to metallic Zn to form Pt–Zn alloy which results in a great increase in the selectivity towards propylene. The formation of the PtZn alloy bimetallic phases can reduce the size of the surface Pt ensembles and suppress the undesired reactions, enhancing the selectivity and stability. Previous study has shown that almost 100% selectivity to isobutene could be obtained over PtZn/C catalysts in isobutane dehydrogenation [18] and it has been attributed to the effect of PtZn alloy. However, the precision of these measurements and calculations does not allow us to affirmatively judge whether there is PtZn alloy over the zinc-doped PtSn catalysts.

### 3.2.4. Electronic effects

CO adsorption was used to determine the effect of zinc on the electronic property of the metal phase. According to some observations in the literature [33,34], the bands in the frequency region 2100–1950  $\text{cm}^{-1}$  can be related to CO linearly bonded to one surface-exposed metal Pt atom. Fig. 4 clearly shows that

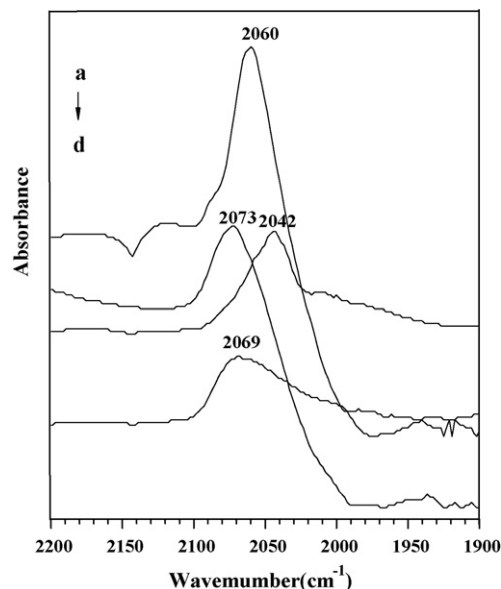


Fig. 4. Comparison of the FTIR spectra of the L CO species on Pt-supported catalysts. (a) Pt/Al; (b) Sn–Pt/Al; (c) Zn–Pt/Al; (d) Zn–Sn–Pt/Al.

the presence of Zn results in a shift of  $-18 \text{ cm}^{-1}$  compared to Pt/Al (from 2060 to 2042  $\text{cm}^{-1}$ ). Likely, the presence of Zn over the Zn–Sn–Pt/Al catalyst also leads to a shift of  $-4 \text{ cm}^{-1}$  with respect to Sn–Pt/Al (from 2073 to 2069  $\text{cm}^{-1}$ ). According to the classic model for the bonding of CO molecules to platinum metal surfaces made by Blyholder [35], a higher metal surface electron density will decrease the CO stretching frequency. Obviously, zinc can increase the electron density of platinum metal surface. The increase in electron density of platinum metal can be the results of both geometrical and chemical effects of the alloying. Firstly, the chemisorption measurements show that addition of Zn to Pt/Al could increase the dispersion of Pt, decreasing the platinum ensembles. For smaller Pt particles, the average number of Pt–Pt bonds per Pt atom is smaller than for the larger particles and a higher metal electron density is available for back bonding into the  $2\pi^*$  orbital of adsorbed CO molecules. This leads to a decrease in the C–O bond strength and a resulting decrease in the CO stretching frequency. Secondly the effect of PtZn alloy may be distinct. Previous studies [36,37] have shown that the alloyed Zn atoms can increase the electron density of Pt sites, leading the IR frequency to move to low frequency. Our analysis of TPR shows that part of Zn species can be reduced to metallic Zn over the Zn–Pt/Al catalyst. The formation of PtZn alloy can also increase the electron density of Pt metal. Although the reduction degree has not been calculated over zinc-doped PtSn catalysts, the possibility of the presence of Pt–Zn alloys should not be easily excluded. Till now, we can see that the formation of PtZn alloy bimetallic phases may also responsible for the high selectivity to propylene over zinc-doped catalysts. The formation of PtZn alloy results in an increase in the electronic density of surface Pt, which will weaken the strength of the Pt–(C=C) bond and promote desorption of olefin. The electronic density increase in metal Pt could further suppress the formation and polymerization of unsaturated coke precursors on the metal and enhance the selectivity and stability of dehy-

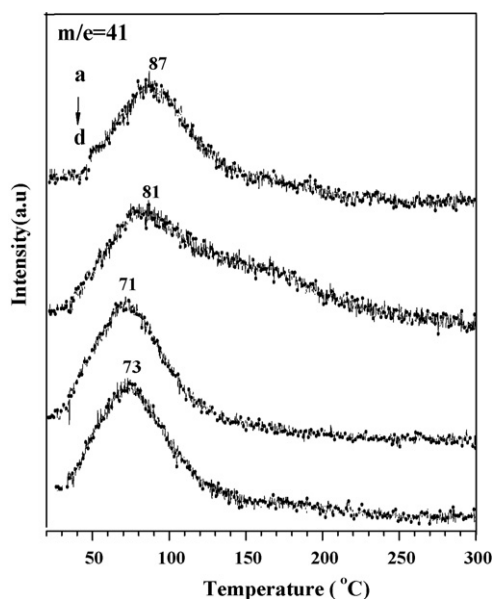


Fig. 5. TPD measurements following propylene adsorption on the catalysts at 20 °C. (a) Pt/Al; (b) Sn–Pt/Al; (c) Zn–Pt/ $\gamma$ -Al<sub>2</sub>O<sub>3</sub>; (d) Zn–Sn–Pt/Al.

drogenation. This point will be verified by the next experiments of C<sub>3</sub>H<sub>6</sub>-TPD and carbon residues analysis.

### 3.2.5. C<sub>3</sub>H<sub>6</sub>-TPD

C<sub>3</sub>H<sub>6</sub>-TPD was used to examine the zinc influence on the property of platinum metal to adsorb propylene. The TPD profiles are presented in Fig. 5. The temperatures of desorption peak can reflect the extent of the interactions between propylene and the metal phase. Addition of zinc to Pt/Al causes the desorption peak shift to lower temperatures, from 87 to 71 °C. A similar picture is given over the zinc-doped PtSn catalyst. The temperatures of desorption peak indicate that Zn weakens the adsorption of propylene and enhances propylene desorption. Promoting propylene desorption can prevent propylene from converting into higher-order dehydrogenation products which are coke precursors. Thereby, a high selectivity towards propylene can be obtained over zinc-doped catalysts. The results of C<sub>3</sub>H<sub>6</sub>-TPD are justly consistent with IR analysis.

### 3.2.6. Analysis of coke

Coke over some used catalysts was characterized by TPO and O<sub>2</sub>-pulse experiments. O<sub>2</sub>-pulse experiment is a special technique used for quantitative analysis of coke. The amount of coke over each used catalyst is shown in Table 5. Fig. 6 shows that one major peak of CO<sub>2</sub> appears over each catalyst, but the temperatures for the major peak are different. The highest temperature peak (450 °C) emerges over the Pt/Al catalyst. Over the Zn–Pt/Al catalyst, low temperature (396 °C) peak for coke burning is observed, which suggests that zinc can reduce the amount of carbon deposition or increase the reactivity of coke. At the same time, coke quantitative analysis (Table 5) clearly shows that the amount of coke over Zn–Pt/Al catalyst (1.5 mg C/g cat) is much lower than that over Pt/Al catalyst (5.3 mg C/g cat). A similar trend appears over zinc-doped PtSn catalysts. However, the amount of coke over zinc-doped PtSn catalyst is also deter-

Table 5

Amount of coke on the catalysts after propane dehydrogenation for 155 min at 576 °C

Catalyst	Coke (mg C/g cat)
Pt/Al	5.3
Sn–Pt/Al	2.7
Zn–Pt/Al	1.5
Zn–Sn–Pt/Al	1.0
Sn–Pt–Zn/Al	1.2
Sn–Zn–Pt/Al	1.3
Pt–SnZn/Al	0.6
SnZn–Pt/Al	3.8

mined by the zinc deposition order. The lowest amount of coke (0.6 mg C/g cat) is observed over the Pt–SnZn/Al catalyst and the highest amount of coke (3.8 mg C/g cat) appears over the ZnSn–Pt/Al catalyst.

Clearly, the presence of zinc can remarkably suppress the formation of coke. The analysis of NH<sub>3</sub>-TPD indicates that over the Zn–Pt/Al catalyst the strong acid sites are poisoned by zinc, which is beneficial to the reduction of coke formation. Other important reasons for the role of zinc in reducing coke can be explained as follows. Firstly, Zn can decrease the size of surface Pt ensembles, thereby inhibiting the formation on the surface of highly dehydrogenated species required for hydrogenolysis, isomerization and coking reactions which require large Pt ensembles. Secondly, the Zn presence brings about an increase in the electronic density of the platinum metal phase, which will weaken the strength of the Pt–(C=C) bond and repulse coke precursors. If we correlate the performance of zinc-doped PtSn catalysts to the amount of coke over these catalysts, we can find that in some cases there exists a great mismatch or disproportion between the amount of carbon formed and the drop in conversion. For instance, deactivation value (20%) for Sn–Pt–Zn(0.5%)/Al is about two times the value (9%) for

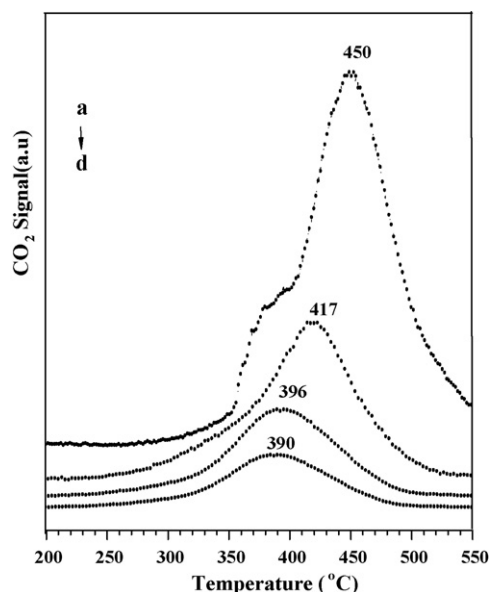


Fig. 6. TPO profiles of coked catalysts (dehydrogenation of propane at 576 °C for 155 min). (a) Pt/Al; (b) Sn–Pt/Al; (c) Zn–Pt/Al; (d) Zn–Sn–Pt/Al.

Zn(0.5%)Sn–Pt/Al, while the amount of coke over SnZn–Pt/Al is three times the value over Sn–Pt–Zn/Al. It indicates that the capacity of zinc-doped PtSn catalysts to resist coke is different. This is likely because the zinc impregnation order could bring about a change in acidity and interactions between active sites, promoters, and support, which result in the different distribution of coke.

#### 4. Conclusions

A great improvement in dehydrogenation selectivity is obtained over both zinc-doped Pt and PtSn catalysts. However, the performance of zinc-doped PtSn catalysts is strongly dependent on the sequence of zinc deposition and the zinc content. High activity and selectivity and the lowest activity loss are obtained over the Zn(0.5%)–Sn–Pt/Al catalyst. The high performance must be related to the low amount of coke and high thermal stability of platinum particles.

Secondly, the presence of zinc results in the change in the properties of the platinum metal phase. Hydrogen chemisorption measurements show that zinc can increase the platinum particles dispersion. The strong surface interactions over zinc-doped PtSn catalysts are revealed by TPR measurements. The zinc existence also changes the electronic environment of platinum metal. An increase in the electronic density of platinum metal is confirmed by CO and propylene adsorption experiments. The change of the platinum metal electronic property must be related to the formation of PtZn alloy. The high electron density of platinum metal can weaken the strength of the Pt–(C=C) bond and promote olefin desorption, then suppressing the formation and polymerization of unsaturated coke precursors on the metal. Coke quantitative and TPO tests also show that the amount of coke can be greatly reduced by zinc.

#### Acknowledgments

The authors would like to acknowledge the contributions made by Yanli He and Jianping Shao in the BET, NH<sub>3</sub>-TPD, C<sub>3</sub>H<sub>6</sub>-TPD, CO-FTIR, and TPO measurements.

#### References

- [1] S.B. Kogan, M. Herskowitz, Catal. Commun. 2 (2001) 179.
- [2] S.D. Migul, A. Castro, O. Scelze, J.L.G. Fierro, J. Soria, Catal. Lett. 36 (1996) 201.
- [3] P. Praserthdam, N. Grisdanurak, W. Yuangsawatdikul, Chem. Eng. 77 (2000) 215.
- [4] H. Liersk, J. Volter, J. Catal. 90 (1984) 96.
- [5] R. Burch, L.C. Garla, J. Catal. 71 (1981) 360.
- [6] F.M. Dautzenberg, J.N. Helle, P. Biloen, W.M.H. Sachtler, J. Catal. 63 (1980) 119.
- [7] O.A. Barias, A. Holmen, E.A. Blekkan, J. Catal. 158 (1996) 1.
- [8] F.B.P.M. Schmal, M.A. Vannice, J. Catal. 160 (1996) 106.
- [9] J.L. Yuan, Appl. Catal. 72 (1991) 33.
- [10] L.Y. Xi, K.J. Klabunde, B.H. Davis, J. Catal. 128 (1991) 1.
- [11] S.M. Stagg, C.A. Quenrini, W.E. Alvarez, D.E. Resasco, J. Catal. 168 (1997) 75.
- [12] J. Llorca, N. Homs, J. Leon, J. Sales, J.L.G. Fierro, P. Ramirez, Appl. Catal. A: Gen. 189 (1999) 77.
- [13] C. Kappenstein, M. Guérin, K. Ližžar, K. Matussek, Z. Pařal, J. Chem. Faraday Trans. 94 (1998) 2463.
- [14] D. Rodriguez, J. Sanchez, G. Arteaga, J. Mol. Catal. A: Chem. 228 (2005) 309.
- [15] D. Akporiaye, S.F. Jensen, U. Olsbye, F. Rohr, E. Rytter, M. Ronnekleiv, A.I. Spjelkavik, Ind. Eng. Chem. Res. 40 (2001) 4741.
- [16] A. Bensaddik, N. Mouaddib, M. Krawczyk, V. Pitchon, F. Garin, G. Maire, Stud. Surf. Sci. Catal. 116 (1998) 265.
- [17] M. Oshimura, A. Kawakami, S. Fujii, Y. Kori, N. Odani, S. Yamaguchi, H. Hosoda, O. Watanabe, A. Miake, O. Okamoto, JP Patent 51054094 (1976).
- [18] J. Silvestre-Albero, J.C. Serrano-Ruiz, A. Sepuřilveda-Escribano, F. Rodriguez-Reinoso, Appl. Catal. A: Gen. 292 (2005) 244.
- [19] M. Consonni, D. Jokic, D.Y. Murzin, R. Touroude, J. Catal. 188 (1999) 165.
- [20] G.R. Wilson, W.K. Hall, J. Catal. 24 (1972) 306.
- [21] J. Freel, J. Catal. 25 (1972) 149.
- [22] S.B. Kogan, H. Schramm, M. Herskowitz, Appl. Catal. A: Gen. 208 (2001) 185.
- [23] R. Burch, J. Catal. 71 (1981) 348.
- [24] H. Armendáriz, A. Guzmán, J.A. Toledo, M.E. Llanos, A. Vázquez, G. Aguilar-Rios, Appl. Catal. A: Gen. 211 (2001) 75.
- [25] O.A. Barias, A. Holmen, E.A. Blekkan, J. Catal. 158 (1996) 4.
- [26] S.W. Park, O.S. Joo, K.D. Jung, H. Kimb, S.H. Han, Appl. Catal. A: Gen. 211 (2001) 81.
- [27] M. Merlen, P. Beccat, J.C. Bertolini, P. Delichere, N. Zanier, B. Didillon, J. Catal. 159 (1996) 178.
- [28] H. Liezke, G. Lietz, H. Spindler, J. Volter, J. Catal. 81 (1983) 8.
- [29] H. Armendáriz, A. Guzmán, J.A. Toledo, M.E. Llanos, A. Vázquez, G. Aguilar-Rios, Appl. Catal. A: Gen. 211 (2001) 75.
- [30] S.R. De Miguel, G.T. Baronetti, A.A. Castro, O.A. Scelza, Appl. Catal. 45 (1988) 61.
- [31] R. Burch, A.J. Mitchell, Appl. Catal. 1 (1983) 121.
- [32] W.S. Yang, L.W. Lin, Y.N. Fan, Catal. Lett. 12 (1992) 267.
- [33] M. Primet, J.M. Basset, M.V. Mathieu, M. Prettre, J. Catal. 29 (1973) 213.
- [34] R. Barth, R. Pitchai, R.L. Anderson, X.E. Verykios, J. Catal. 116 (1989) 61.
- [35] G. Blyholder, J. Phys. Chem. 68 (1964) 2772.
- [36] F. Bocuzzi, A. Chiorino, G. Ghiotti, F. Pinna, G. Strukul, R. Tessari, J. Catal. 126 (1990) 387.
- [37] F. Bocuzzi, A. Chiorino, E. Guglielminotti, Surf. Sci. 368 (1996) 269.